Neutral Density Response to Solar Flares at Mars

E. M. B. Thiemann[1], F. G. Eparvier[1], L. A. Andersson[1], C. M. Fowler[1], W. K. Peterson[1], P. R. Mahaffy[2], S. L. England[3], D. E. Larson[3], D. Y. Lo[4], N. M. Schneider[1], J. I. Deighan[1], W .E. McClintock[1], B. M. Jakosky[1]

[1]Laboratory For Atmospheric and Space Physics, University of Colorado, 1234 Innovation Dr., Boulder, CO 80303

[2]NASA Goddard Space Flight Center, 8800 Greenbelt Rd, Greenbelt, MD 20771

[3]Space Sciences Laboratory, University of California-Berkeley, Berkeley, CA 94720

[4]Lunar and Planetary Laboratory, University of Arizona, Tuscon, AZ 85721

Corresponding Author: E. M. B. Thiemann, thiemann@lasp.colorado.edu

A Manuscript Submitted to Geophysical Research Letters

September 24, 2015

Accepted Article

This article has been accepted for publication and undergone full peer review but has not been through the copyediting, typesetting, pagination and proofreading process which may lead to differences between this version and the Version of Record. Please cite this article as doi: 10.1002/2015GL066334

©2015 American Geophysical Union. All rights reserved.

Abstract

First direct observations of heating of the Mars neutral atmosphere by solar flares are presented in this study. Solar flares were detected using the Extreme Ultraviolet Monitor (EUVM) on board the Mars Atmosphere and Volatile Evolution (MAVEN) spacecraft, and upper atmospheric temperature enhancements were determined by changes in the density scale height of Argon (Ar) made by the Neutral Gas Ionizing Mass Spectrometer (NGIMS) also on board MAVEN. We analyzed 14 M-Class or greater flares that occurred during the early part of the MAVEN mission in addition to a 30 day period of high flare activity during May 2015. We report that the Mars day-side upper atmosphere shows significant heating near the flare soft x-ray peak; and it responds and recovers rapidly to heating from M-class or larger flares. In addition, we present atmospheric density versus altitude profiles that were taken near the soft x-ray peak of two flares.

Key Points:

1. First observations of neutral heating at Mars due to solar flares are reported.

2. The upper atmosphere shows significant heating near the flare soft x-ray peak.

3. The Mars atmosphere responds and recovers rapidly to heating from M-class flares.

Accepted Article

©2015 American Geophysical Union. All rights reserved.

1.0 Introduction

Solar flares are transient events in the solar corona that result in emissions which span the electromagnetic spectrum from x-ray to radio wavelengths [Aschwanden, 2005]. The wavelength range from .1-121.6 nm, which we define here as the Extreme Ultraviolet (EUV), is of particular interest because it is highly variable and the primary energy source for the upper atmospheres of terrestrial planets [Schunk and Nagy, 2009]. Solar flares are seen at Earth and Mars as a transient enhancement of ionizing photon flux, and the photon energy is transformed into chemical and kinetic energy upon absorption which is ultimately dissipated as heat [Roble, 1995]. Solar flares are often ranked according to the NOAA flare scale which designates flares as C, M or X –class for Common, Moderate or Extreme corresponding to the flare's intensity. When used in this letter, the NOAA scale will always correspond with irradiance at 1 AU. At solar max (min), 2000 (300) C class flares, 300 (20) M class flares and 10 (<1) X class flares occur per year [Yashiro *et al.*, 2005]. Because of their relative frequency, observations of flare effects resulting from M-class flares may have a greater cumulative effect on the Mars atmosphere even though the effects may be less dramatic than their larger X-class counterparts.

Mars thermospheric neutral densities and temperatures are the result of balancing the absorption of solar radiation with thermal conduction and radiative cooling processes which are poorly understood, but have become better constrained more recently [e.g. Bougher *et al.*, 2009; Bougher *et al*., 2015]. Changes in the thermosphere in response to EUV variability provides an opportunity to better constrain these processes at Mars. *Forbes et al.* (2006) reported density changes of the Mars thermosphere at 390 km due to solar rotational variability and compared them with 400 km density measurements at Earth, but no measurements have yet been reported on the Mars thermosphere response to solar flares. Further, prior measurements of the EUV response of the Mars thermosphere reported by

©2015 American Geophysical Union. All rights reserved.

Accepted Article

Forbes et al. (2007) were constrained to a particular height (390 km); because the thermospheric mixing ratios change with height, density versus height profiles can provide insight into non-equilibrium processes.

The Earth and Mars upper thermospheres share similar neutral densities and both have O as the dominant neutral species [Schunk and Nagy, 2009] so comparisons between the two can be insightful. *Sutton et al.* (2006) showed neutral density enhancements at 400 km corresponding with two large solar flares at Earth, and *Le* (2011) has subsequently done an analysis of the neutral density response at 400 km (Earth) to all X-class solar flares between 2001 and 2006. *Liu et al.* (2007) compared the thermosphere and ionosphere responses for one large flare at Earth and showed that both the neutral density in the thermosphere and electron density in the ionosphere respond immediately to a solar flare although the large heat capacity of Earth's neutral atmosphere causes a delay between the peak neutral density and the peak flare irradiance. Because of the relatively tenuous atmosphere at Mars and corresponding smaller heat capacity, we expect the Mars thermosphere to respond more quickly and to be more sensitive to solar flares.

Flare effects on the Mars ionosphere have also been observed [e.g. Mendillo *et al.*, 2006], but the observations have been limited to measurements of the ionization process via radio occultation experiments done by the Mars Global Surveyor (MGS) Radio Science experiment [Hinson *et al.*, 1999]. The radio occultation technique can detect electron density enhancements that are the result of flare induced ionization, but is not capable of resolving the neutral density. Liu *et al.* (2007) showed spatial and temporal differences in the thermosphere and ionosphere responses at Earth, demonstrating the need for measurements of both neutral and electron density response to solar flares to fully characterize the impact flares have on the upper atmosphere.

©2015 American Geophysical Union. All rights reserved.

Accepted Article

In this letter, we report the first observations of changes in the neutral constituents of the Mars thermosphere as a result of solar flares. Unlike similar measurements previously made at Earth, these measurements span 150 km in height providing solar flare affected vertical profiles of neutral density previously unavailable at any terrestrial planet. We report neutral density and temperature results for three events using the EUVM [Eparvier *et al.*, 2014] and NGIMS [Mahaffy *et al.*, 2014] instruments on board MAVEN [Jakosky *et al.*, 2015].

2.0 Data and Sources

The data for this study are provided by EUVM [Eparvier *et al*., 2015] and NGIMS [Mahaffy *et al*., 2015] onboard the MAVEN [Jakosky *et al.*, 2011] spacecraft. MAVEN has a highly eccentric orbit with periapsis near 150 km and apoapsis near 6200 km with a 4.5 hour period. The orbit also precesses to allow atmospheric sampling across all local times. This allows for in-situ measurements of the Mars upper atmosphere down to approximately 150 km every orbit, covering the entire planet local time in approximately one earth year. EUVM samples 3 solar EUV bands at 1 second time cadence, but is typically pointed away from the sun every other periapsis to accommodate other instrument operations. Data gaps also occur regularly due to eclipses when Mars is along the MAVEN-Sun line-of-site. The EUVM Level 2 version (v) 3, Revision (r) 1 data product consists of calibrated irradiances for the 3 bands at one-minute time cadence and was used to identify flares and classify their magnitude. The EUVM 0-7 nm band is calibrated for a non-flaring solar spectrum. Therefore, when discussing EUVM 0-7 nm flare measurements, it is more precise to use a unitless Soft X-ray (SXR) index. NGIMS samples neutral Ar, CO_2, N_2, He every orbit and the neutrals; O, CO, NO; and ions; O_2^+, CO_2^+ NO^+, O^+; on alternating orbits at a 4 second time cadence. The Level 2 v4, r1 and r3 NGIMS products were used to find neutral density as a function of height.

©2015 American Geophysical Union. All rights reserved.

Accepted Article

In addition to solar flare heating, the upper atmosphere of Mars can be heated by other drivers such as atmospheric wave activity [e.g. Medvedev & Yiğit, 2012] which transfer energy from atmospheric perturbations, and Solar Energetic Particles (SEP) [Leblanc *et al.*, 2002]. Therefore, these drivers should be ruled out if the observed heating is to be attributed to a particular flare. The Imaging Ultraviolet Spectrograph (IUVS) [McClintock *et al.*, 2014] on-board MAVEN can be used to characterize tidal wave amplitudes, and NGIMS can be used to measure the gravity wave amplitudes [Yiğit *et al.*, this issue.]; the Solar Energetic Particle (SEP) instrument [Larson *et al.*, 2015], also on-board MAVEN, can be used to measure SEP activity.

3.0 Methodology

From all flares observed by MAVEN EUVM, we selected 13 flare events based on the following criteria: 1) The measured EUVM 0-7 nm SXR Index exceeded 2 which corresponds approximately with an M2 GOES class flare, and 2) the MAVEN periapsis occurred on the dayside of Mars which ensures a solar zenith angle (SZA) below 90° during either periapsis ingress or egress. For each event, we only considered the orbit leg with the lower average SZA based on the assumption that any flare induced effects would be more pronounced near the sub-solar point. The 13 flare events that meet these criteria are listed in Table 1 with their corresponding SXR irradiance, delay time between the SXR peak and MAVEN periapsis, percent temperature increase, and the SZA at periapsis. The only flare that does not meet the aforementioned criteria is Flare 14 which coincides with the largest temperature increase observed in this study.

Assuming diffusive equilibrium, the atmospheric neutral density profile varies logarithmically and is proportional to $e^{-\frac{z\,mg}{kT}}$ where z is the height above some reference, m is the particle mass, g is the gravitational acceleration, k is Boltzman's constant and T is the

©2015 American Geophysical Union. All rights reserved.

temperature [Shunk and Nagy, 2009]. As the temperature increases, the density at a fixed height also increases. This relationship allows for extrapolation of the temperature by measuring the density profile and fitting the scale height, $H=kT/mg$ which is used in the following analysis.

Although CO_2 is the dominant neutral constituent in the Mars atmosphere below approximately 225 km and O is the dominant species above 225 km, these two species are subject to chemical processes that can result in a non-diffusive variation of density with height. Ar provides a much cleaner signal for estimating thermospheric temperature because the density dependence on height is driven primarily by diffusion due to its inert nature. Also, because Ar is inert, it is not subject to inner-instrument chemical reactions which can compromise the calibration. For these reasons, our analysis used NGIMS Ar density observations between 170 km and 300 km unless otherwise stated, and assumed diffusive equilibrium. Several periapsis passes before and after the flare were examined to determine ingress and egress Ar scale heights (H). The scale heights were inverted for temperature (T). For the set of temperatures excluding the orbit immediately after the flare, the mean and standard deviation were calculated to determine a baseline of the atmospheric temperature and variability for non-flaring conditions. The temperature for the post-flare orbit was then compared to the non-flare mean and standard deviation to look for statistically significant changes.

If significant heating was detected, we searched for other sources of heating including SEP heating using the SEP instrument and atmospheric wave heating using the NGIMS and IUVS instruments.

Accepted Article

©2015 American Geophysical Union. All rights reserved.

4.0 Observations of Flare Induced Atmospheric Heating At Mars

Atmospheric temperatures exceeding two standard deviations of the 3-day orbit mean from the events in Table 1 were observed during orbits after Flares 1, 12 and 14. These events are unique with regard to the others in Table 1 in that the flares were in-progress during the neutral density measurements below 300 km. We review Flares 12 and 14 in detail below; but omit Flare 1 due to space constraints, and because Flare 1 coincided with a period of high solar activity with many flares and a large CME in addition to an encounter with Comet Siding Spring, all of which result in a highly disturbed atmosphere making it difficult to analyze any one particular event.

4.1 Overview of Thermospheric and Solar Soft X-ray Variability

The two right-most columns in Table 1 are the change in temperature for the post-flare orbit from the pre-flare orbit temperature (ΔT) calculated at two differing altitude ranges. The column labeled ΔT contains temperatures derived from 170-270 km, and the column labeled *Top-Side* ΔT contains temperatures derived from 200-270 km to suppress forcing the lower atmosphere. On average, both of these values should be near zero. Taking the mean of these columns yields a temperature change of 28.4 K and 55.3 K for the ΔT and *Top-Side* ΔT values, respectively. If we omit Flare 14 to prevent its large value from skewing the average, we find the means to be 16.9 K and 36.3 km for the ΔT and *Top-Side* ΔT values, respectively. These results suggest the upper thermosphere is more sensitive to flare induced heating and/or less sensitive to other forcing that can overshadow the flare-induced changes. Taking into consideration the column labeled *Delay,* which is the time that has passed since the flare peaked before the temperature measurements were made, Table 1 shows that all flares which peaked less than 1.5 hours prior to temperature measurements show an increase in

Accepted Article

©2015 American Geophysical Union. All rights reserved.

temperature, suggesting that the Mars upper thermosphere responds and recovers quickly to flare heating.

Figures 1 (a) and (b) are the 200-270 km temperatures for the out-bound orbits and the corresponding SXR Index for the period from 26 April 2015 and 26 May 2015 where the SZA varies gradually from 15° to 58°. We used the data in Figure 1 (a) to calculate the Mean Daily Temperature Variability (MDTV) which we define as the 6 orbit (~27 hours) running mean of the absolute value of ΔT. We define the Mean Daily Flare Variability (MDFV) as the 6 orbit running mean of the maximum change in the SXR over each orbit. The (Pearson) correlation coefficient between the MDTV and MDFV is equal to .56, and it is equal to .75 if only the values corresponding with the MDTV being greater than its mean value are considered. This suggests that solar flares are a driver of larger than average temperature swings from 200-270 km.

4.2 Flare 12 Case Study

Flare 12 occurred on 24 March 2015 coinciding with an atmospheric temperature increase during the in-bound portion of the following orbit equal to 3.1 time the standard deviation of the temperature for the surrounding three days (σ_{3d}). Figure 2 shows (a) the EUVM SXR index, (b) the 170-300 km temperature for the flare orbit (red) and surrounding orbits, (c) the orbit-to-orbit temperature changes, (d) the in-bound and out-bound density profiles for the 3 days considered with the post-flare peak orbit shown in red. The SZA and latitude are shown in the top horizontal axis of (d). The MAVEN periapsis was at 17.1˚ N and 15:07 Local Solar Time (LST). MAVEN entered periapsis near the subsolar point, flying north and towards the dusk terminator. The EUVM instrument was pointed away from the sun during this periapsis due to routine spacecraft operations preventing the SXR peak from being measured. We estimate from the data shown in Figure 2(a) that MAVEN periapsis occurred

©2015 American Geophysical Union. All rights reserved.

Accepted Article

at, or very near, the SXR peak time. NGIMS and EUVM data are available for orbits preceding the flare and the orbit nearest the flare peak. However, there are no NIGMS or EUVM data available for the following 12 orbits because IUVS was performing a stellar occultation campaign which had spacecraft pointing requirements that prevented NGIMS and EUVM from making measurements. The lower bound of the SXR Index peak is given by the first available measurements coming out of periapsis and is 3.1.

At the time of writing, IUVS data was not available to determine tidal wave activity. However, because tidal wave heating is expected to be gradual (varying over a period of days), we assume that it is not the source of the abrupt change in temperature during Orbit 932. Gravity wave activity is considered to be moderate.

4.3 Flare 14 Case Study

Flare 14 occurred on 4 May 2015 and is associated with with an atmospheric temperature increase during the following orbit equal to $4.1\sigma_{3d}$. Figure 3 shows NGIMS and EUVM data for this event arranged in the same order as in Figure 2 with the addition of solar Lyman-α data in 3(a). The MAVEN periapsis was at 3˚ N and 10:46 LST. MAVEN entered periapsis flying North and towards the subsolar point and remained in the pre-noon sector while below 353 km, passing through 11:56 LST at 363 km during the out-bound leg. The period of time covered by Figures 3 (a) and (b) is included in Figure 1. The key difference being that Figure 1 derives temperatures from 200-270 km rather than 170-300 km. Note that the two largest values of ΔT in Figure 1(a) occur during Orbits 1150 and 1152 which are shown in Figures 3 (a) and (b) in more detail.

IUVS data were not available for this event for detailed tidal wave activity, but we ignore the contribution of tidal activity again based on the assumption that its contribution will be gradual. Gravity wave activity is the smallest for this orbit of Flares 1,12 and 14, and the

©2015 American Geophysical Union. All rights reserved.

Accepted Article

SEP instrument shows relatively quiet particle environment conditions although there is an enhancement of solar energetic particles flux between orbits 1153 and 1154.

4.4 Discussion

The unifying factor between Flares 1, 12 and 14 in Table 1, each of which resulted in significant heating, is that the flares occurred during the temperature measurements. Other flares were observed with comparable or greater magnitude to these three but typically an hour or more elapsed before NGIMS took atmospheric measurements. This suggests that the Mars upper atmosphere temperature responds to solar flares quickly and recovers quickly after the flare has ended which is consistent with a low density, and hence low heat capacity, atmosphere. Note that the reason Flare 1 corresponded with a smaller temperature increase than Flares 12 and 14, even through it had the largest SXR flux, is likely related to it having the largest SZA. This is consistent to model/measurement comparisons by Pawlowski and Ridley (2008) and Qian et al. (2011) who show the flare related density enhancements to be highest at the sub-solar point and decrease with increasing SZA.

Earth's thermosphere also shows a rapid response to solar flares. For example, *Liu et al.* (2007) reported a near instantaneous increase in neutral density, and implicitly temperature, at 400 km, showing approximately a 20% enhancement during the solar SXR peak. This is similar to Flare 12 which also shows that the Mars atmosphere heats rapidly in response to solar flares, and a 66% enhancement of the Ar density at 250 km at the approximate time of the SXR peak. When considering the atmospheric response time, it is also important to note that many EUV emissions peak prior to the soft x-ray peak and *Chamberlin et al.* (2008) showed that many EUV emission lines are proportional to the time derivative of the SXR emissions; this is known as the Neupert Effect [Neupert 1968, 1989]. Therefore, the SXR peak typically occurs after the time of peak EUV emission, and what may appear to be an

©2015 American Geophysical Union. All rights reserved.

Accepted Article

instantaneous response to SXR irradiance may be a delayed response to another portion of the EUV spectrum.

Another similarity between these Mars observations and previously reported Earth flare thermospheric effects is the apparent dependence on the spectral content of a flare on its ability to effect an atmosphere. Looking at Figures 3 (a) and (b), the SXR Index is not exceptionally high for the flare preceding orbit 1152; however, the 121.6 nm flux is the highest for the flares shown. It has been reported at Earth that solar EUV emissions, much of which originates from denser solar plasma than SXR emissions, are a significant contributor to flare induced atmospheric heating [Qian *et al*. 2010]. Le et al. (2012) compared neutral density enhancements for X-class flares at Earth and showed the time-integrated 26-34 nm EUV irradiance to be better correlated with atmospheric density enhancements than the peak SXR, peak EUV or time integrated SXR irradiance. This is because many EUV lines tend to be optically thick (in the solar atmosphere) and are sensitive to the flare-site geometry whereas optically thin emissions such as the 0-7 nm band are not [Chamberlin *et al*., 2007]. It follows that optically thin emissions such as the 0-7 nm band are not the best indicators for the extent a particular flare can heat an atmosphere. On the other hand, emissions from similar densities in the solar atmosphere are well correlated [Chamberlin *et al*., 2007]. Therefore, 121.6 nm, being an optically thick emission, should be a better predictor of the intensity of other optically thick emissions and, hence, the potential for a flare to heat an atmosphere. These considerations may help explain why the flare preceding orbit 1150 which met the initial search criteria of having SXR Index above 3 resulted in no statistically significant heating whereas the flare preceding orbit 1152, which had significant 121.6 nm flux, corresponded with substantial atmospheric heating. Another mechanism which can cause atypically large EUV flux is the EUV Late Phase (ELP) first reported by Woods et al (2011). The ELP is a second peak in some EUV emissions occurring many minutes or even

©2015 American Geophysical Union. All rights reserved.

Accepted Article

hours after the SXR peak and is associated with eruptive events. The flare shown in Figure 2(a) at ~1151.5 was shown by SOHO LASCO imagery to have a CME associated with it, and therefore could have had an ELP contributing to the total EUV flux 2 hours later. Note that EUVM is not capable of detecting the ELP.

There are also similarities between the three events with the altitudes where the density is increased. None of the events show significant density increases below approximately 210 km for the legs with the lowest SZA. This altitude also corresponds approximately with the height where O overtakes CO_2 as the major neutral species. We speculate that lack of density enhancements below ~210 km may be due to the lower atmosphere being more efficient at dissipating heat via CO_2 cooling. A similar effect was shown by Qian et al. (2010) at Earth who showed that NO cooling can suppress flare-induced heating at lower altitudes in Earth's thermosphere.

5.0 Conclusion

Solar flares provide a quantifiable transient perturbation to the Mars atmosphere from its equilibrium state which can be used to better constrain atmospheric models; and a detailed modeling paper using the Mars Global Ionosphere-Thermosphere Model [Bougher *et al.*, 2015] will follow this letter. The utility of using solar flares to advance our understanding of the Earth's thermosphere has been recognized in the past decade with *Sutton et al.* (2007) stating that "(solar flare effects) provide new opportunities for the testing and validation of models over time scales similar to those of basic mechanisms governing the thermosphere response, such as thermal conduction, radiative cooling, and restoration to diffusive equilibrium". The same arguments apply to Mars, but with more urgency, given the sparse set of observations of the Mars atmosphere. Although the set of flare heating observations presented here is limited to primarily moderate events, they include observations at a diverse

©2015 American Geophysical Union. All rights reserved.

Accepted Article

set of SZAs (with Flares 1, 12 and 14 nearly evenly spaced from 21˚ to 68˚) and a diverse set of flare intensities, and show a neutral density structure that presents new challenges that can be immediately undertaken by the broader heliophysics community.

6.0 Acknowledgements

The MAVEN project is supported by NASA through the Mars Exploration Program. S.L.E.'s contribution was supported by NASA grant NNX13AO36G. MAVEN data is publically available through the NASA Planetary Data System: https://pds.nasa.gov/. E.M.B.T. would like to thank S. Bougher and X. Fang for their helpful discussions regarding this study. We would like to thank the anonymous reviewers for their feedback which we believe improved this study overall.

7.0 References

Aschwanden, M. (2006). *Physics of the solar corona: an introduction with problems and solutions*. Springer Science & Business Media.

Bougher, S. W., McDunn, T. M., Zoldak, K. A., & Forbes, J. M. (2009). Solar cycle variability of Mars dayside exospheric temperatures: Model evaluation of underlying thermal balances. *Geophysical Research Letters*, 36(5).

Bougher, S. W., Pawlowski, D., Bell, J. M., Nelli, S., McDunn, T., Murphy, J. R., ... & Ridley, A. (2015). Mars Global Ionosphere-Thermosphere Model: Solar cycle, seasonal, and diurnal variations of the Mars upper atmosphere. *Journal of Geophysical Research: Planets*, *120*(2), 311-342.

Chamberlin, P. C., Woods, T. N., & Eparvier, F. G. (2007). Flare irradiance spectral model (FISM): Daily component algorithms and results. *Space Weather*, *5*(7).

©2015 American Geophysical Union. All rights reserved.

Accepted Article

Chamberlin, P. C., Woods, T. N., & Eparvier, F. G. (2008). Flare irradiance spectral model (FISM): Flare component algorithms and results. *Space Weather*, *6*(5).

Dean, J. A. (1985). Lange's handbook of chemistry.

Eparvier, F. G., Chamberlin, P. C., Woods, T. N., & Thiemann, E. M. B. (2015). The Solar Extreme Ultraviolet Monitor for MAVEN. *Space Science Reviews*, 1-9.

Forbes, J. M., Bruinsma, S., & Lemoine, F. G. (2006). Solar rotation effects on the thermospheres of Mars and Earth. *Science*, *312*(5778), 1366-1368.

Hinson, D. P., Simpson, R. A., Twicken, J. D., Tyler, G. L., & Flasar, F. M. (1999). Initial results from radio occultation measurements with Mars Global Surveyor. *Journal of Geophysical Research: Planets (1991–2012)*, *104*(E11), 26997-27012.

Jakosky, B. M., Lin, R. P., Grebowsky, J. M., Luhmann, J. G., Mitchell, D. F., Beutelschies, G., & Lefèvre, F. (2015). The Mars Atmosphere and Volatile Evolution (MAVEN) Mission. *Space Science Reviews*, 1-46.

Larson, D., Lillis, R. J., Rahmati, A., Dunn, P., Cravens, T., Curtis, D., & Connerney, J. (2015, April). The Solar Energetic Particle experiment on MAVEN: first results. In AAS/AGU Triennial Earth-Sun Summit (Vol. 1, p. 30506).

Le, H., Liu, L., & Wan, W. (2012). An analysis of thermospheric density response to solar flares during 2001–2006. *Journal of Geophysical Research: Space Physics* (1978–2012), 117(A3).

Leblanc, F., Luhmann, J. G., Johnson, R. E., & Chassefiere, E. (2002). Some expected impacts of a solar energetic particle event at Mars. *Journal of Geophysical Research: Space Physics (1978–2012)*, *107*(A5), SIA-5.

©2015 American Geophysical Union. All rights reserved.

Accepted Article

Liu, H., Lühr, H., Watanabe, S., Köhler, W., & Manoj, C. (2007). Contrasting behavior of the thermosphere and ionosphere in response to the 28 October 2003 solar flare. *Journal of Geophysical Research: Space Physics (1978–2012)*, *112*(A7).

Lo, D. Y., *et al.*, Tides in the Martian Atmosphere as Observed by MAVEN IUVS, this issue.

Mahaffy, P. R., Benna, M., King, T., Harpold, D. N., Arvey, R., Barciniak, M., ... & Nolan, J. T. (2014). The Neutral Gas and Ion Mass Spectrometer on the Mars Atmosphere and Volatile Evolution Mission. *Space Science Reviews*, 1-25.

Mahajan, K. K., Lodhi, N. K., & Singh, S. (2009). Ionospheric effects of solar flares at Mars. *Geophysical Research Letters*, *36*(15).

Medvedev, A. S., & Yiğit, E. (2012). Thermal effects of internal gravity waves in the Martian upper atmosphere. *Geophysical Research Letters*, *39*(5).

Mendillo, M., Withers, P., Hinson, D., Rishbeth, H., & Reinisch, B. (2006). Effects of solar flares on the ionosphere of Mars. *Science*, *311*(5764), 1135-1138.

Neupert, W. M. (1968). Comparison of solar X-ray line emission with microwave emission during flares. *The Astrophysical Journal*, *153*, L59.

Neupert, W. M. (1989). Transient coronal extreme ultraviolet emission before and during the impulsive phase of a solar flare. *The Astrophysical Journal*, *344*, 504-512.

Pawlowski, D. J., & Ridley, A. J. (2008). Modeling the thermospheric response to solar flares. *Journal of Geophysical Research: Space Physics* (1978–2012), 113(A10).

Qian, L., Burns, A. G., Chamberlin, P. C., & Solomon, S. C. (2010). Flare location on the solar disk: Modeling the thermosphere and ionosphere response. *Journal of Geophysical*

Accepted Article

©2015 American Geophysical Union. All rights reserved.

Research: Space Physics (1978–2012), *115*(A9).

Qian, L., Burns, A. G., Chamberlin, P. C., & Solomon, S. C. (2011). Variability of thermosphere and ionosphere responses to solar flares. *Journal of Geophysical Research: Space Physics (1978–2012)*, *116*(A10).

McClintock, W. E., Schneider, N. M., Holsclaw, G. M., Clarke, J. T., Hoskins, A. C., Stewart, I., & Deighan, J. (2014). The imaging ultraviolet spectrograph (IUVS) for the MAVEN mission. Space Science Reviews, 1-50.

Schunk, R., & Nagy, A. (2009). *Ionospheres: physics, plasma physics, and chemistry*. Cambridge university press.

Sutton, E. K., Forbes, J. M., Nerem, R. S., & Woods, T. N. (2006). Neutral density response to the solar flares of October and November, 2003. *Geophysical Research Letters*, *33*(22).

Thiemann, E., Eparvier, F. G., & Chamberlin, P. C. (2014, December). FISM-P: A Model of the Vacuum Ultraviolet Irradiance Spectrum for Atmospheric Studies at Mars and Beyond. In *AGU Fall Meeting Abstracts* (Vol. 1, p. 3940).

Yashiro, S., Akiyama, S., Gopalswamy, N., & Howard, R. A. (2006). Different power-law indices in the frequency distributions of flares with and without coronal mass ejections. *The Astrophysical Journal Letters*, *650*(2), L143.

Yiğit, E., England, S. L., Liu, G., Medvedev, A. S., Mahaffy, P. R., Kuroda, T. (2015). High-altitude gravity waves in the Martian thermosphere observed by MAVEN/NGIMS and modeled by a gravity wave scheme. Geophysical Research Letters, Submitted to this iss

Accepted Article

©2015 American Geophysical Union. All rights reserved.

Table 1. Candidate Flares for Heating

Number	Flare Peak Time (UT)	Peak SXR Index	Delay[1] (Hrs)	Periapisis SZA (˚)	ΔT.[3] (K)	Top-side ΔT[4] (K)
1	19 Oct 2014 5:08	12.5	0.75	68.5	58.43	62.46
2	20 Oct 2014 16:40	9	1.3	68.4	34.93	41.46
3	22 Oct 2014 2:10	7	No NGIMS	68.5	No NGIMS	No NGIMS
4	11/16/2014 17:50	4.9	2.66	82.6	31.7	86.05
5	28 Feb 2014 4:55	2.6	2.08	87.8	5.13	-2.35
6	1 Mar 2015 12:45	11.5	1.5	86.1	-13.98	-6.9
7	6 Mar 2015 6:00	>2.6	1	77.8	12.63	9.2
8	7 Mar 2015 22:35	8.6	1	76.3	11.76	19.4
9	10 Mar 2015 00:00	3.3	1.5	71.1	-14.72	-2.8
10	17 Mar 2015 14:00	>2.4	No NGIMS	59.3	No NGIMS	No NGIMS
11	19 Mar 2015 22:00	3.2	2.5	56.2	-10.4	-23.9
12	3/24/2015 8:45	>3.1	0	49.1	64.4	68.8
13	4 May 2015 3:05	3	.58	22.3	5.7	147.9
14	4 May 2015 12:10	1.16	.33	22.3	155.3	263.9

1. Difference between periapsis and flare peak times.

2. Change in temperature of post flare orbit from three-day mean.

3. Change in temperature of post-flare orbit from pre-flare orbit measured from 170-270 km.

4. Change in temperature of post-flare orbit from pre-flare orbit measured from 200-270 km.

Accepted Article

©2015 American Geophysical Union. All rights reserved.

Accepted Article

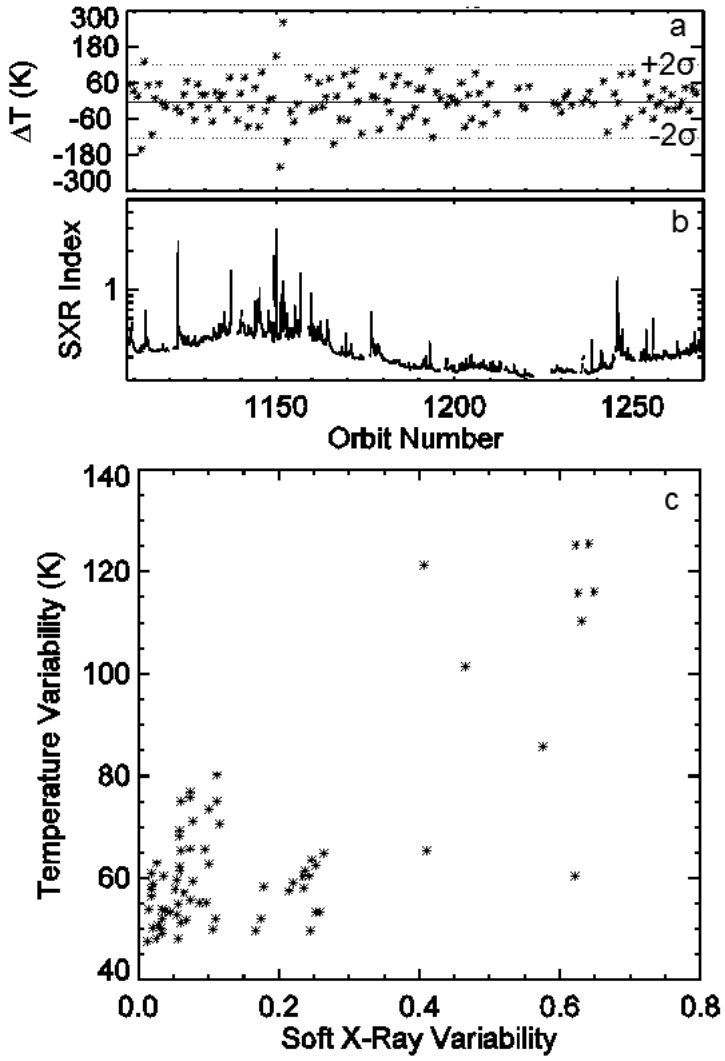

Figure 1. Thermosphere and Soft X-Ray Variability from April 26- May 26, 2015. (a) The 200-270 km orbit-to-orbit temperature change *(with the 2X standard-deviation value indicated),* (b) the SXR index, (c) scatter plot of the excess daily temperature variability and daily SXR variability.

©2015 American Geophysical Union. All rights reserved.

Accepted Article

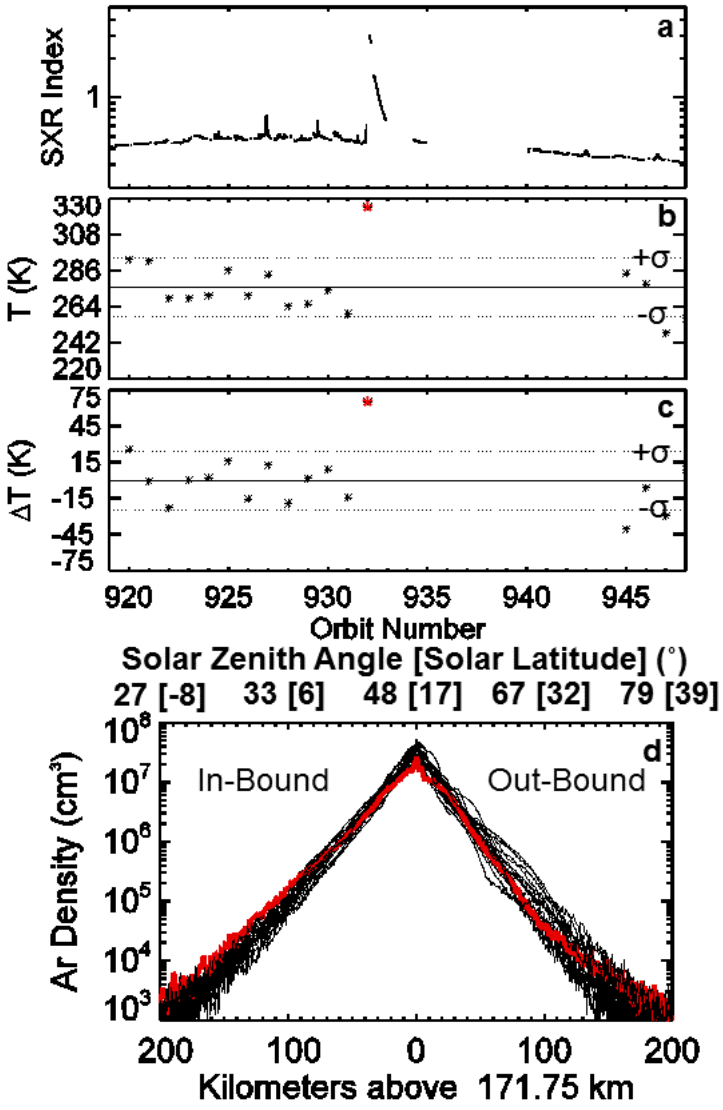

Figure 2. March 24, 2015 flare heating observations. (a) The EUVM 0-7 nm SXR index, (b) the Ar derived 170-300 km temperature for the flare orbit (red) and surrounding orbits, (c) the orbit-to-orbit change in temperature (with the standard deviation value indicated), and (d) the in-bound (out-bound) Ar density profiles for the 3 days considered with the post-flare orbit shown in red. The SZA and solar latitude are shown in the top horizontal axis of (d).

©2015 American Geophysical Union. All rights reserved.

Accepted Article

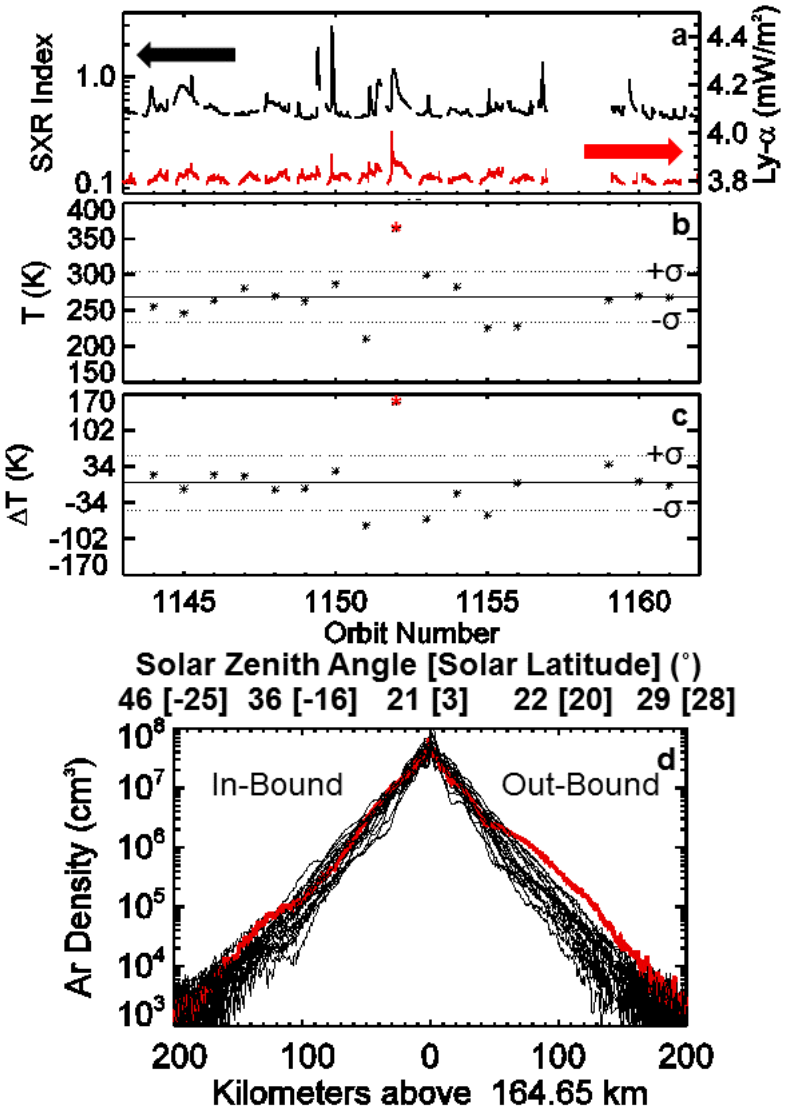

Figure 3. May 4, 2015 flare heating observations. Same layout as Figure 2 with the addition of EUVM Solar Lyman α irradiance included in (a).

©2015 American Geophysical Union. All rights reserved.